IEEE Access
Multidisciplinary | Rapid Review | Open Access Journal

Received June 10, 2018, accepted August 8, 2018, date of publication August 13, 2018, date of current version September 7, 2018.

Digital Object Identifier 10.1109/ACCESS.2018.2865122

Application of Neural-Like P Systems With State Values for Power Coordination of Photovoltaic/Battery Microgrids

TAO WANG[1,2,3], (Member, IEEE), JUN WANG[1,2,3], JUN MING[4], ZHANG SUN[1,2,3], CHUANXIANG WEI[5], CHUN LU[6], AND MARIO J. PÉREZ-JIMÉNEZ[7]

[1]School of Electrical Engineering and Electronic Information, Xihua University, Chengdu 610039, China
[2]Sichuan Province Key Laboratory of Power Electronics Energy-Saving Technologies & Equipment, Xihua University, Chengdu 610039, China
[3]Key Laboratory of Fluid and Power Machinery, Ministry of Education, Xihua University, Chengdu 610039, China
[4]State Grid Zigong Electric Power Supply Company, Zigong 643000, China
[5]State Grid Nanchong Electric Power Supply Company, Nanchong 637000, China
[6]Ceit and Tecnun, University of Navarra, 20018 San Sebastian, Spain
[7]Research Group on Natural Computing, Department of Computer Science and Artificial Intelligence, University of Sevilla, 41012 Sevilla, Spain

Corresponding author: Jun Wang (wj.xhu@hotmail.com)

This work was supported in part by the Chunhui Project Foundation of the Education Department of China under Grant Z2016143, in part by the National Natural Science Foundation of China under Grant 61472328, Grant 61703345, and Grant 51607146, in part by the International Cooperation Project of Chengdu Science and Technology Bureau under Grant 2016-GH02-00111-HZ, in part by the Key Fund Project of the Sichuan Provincial Education Department under Grant 18ZA0459, in part by the Key Scientific Research Fund Project of Xihua University under Grant Z17108, and in part by the Innovation Fund for Graduate Students of Xihua University under Grant ycjj2017059.

ABSTRACT The power coordination control of a photovoltaic/battery microgrid is performed with a novel bio-computing model within the framework of membrane computing. First, a neural-like P system with state values (SVNPS) is proposed for describing complex logical relationships between different modes of Photovoltaic (PV) units and energy storage units. After comparing the objects in the neurons with the thresholds, state values will be obtained to determine the configuration of the SVNPS. Considering the characteristics of PV/battery microgrids, an operation control strategy based on bus voltages of the point of common coupling and charging/discharging statuses of batteries is proposed. At first, the SVNPS is used to construct the complicated unit working modes; each unit of the microgrid can adjust the operation modes automatically. After that, the output power of each unit is reasonably coordinated to ensure the operation stability of the microgrid. Finally, a PV/battery microgrid, including two PV units, one storage unit, and some loads are taken into consideration, and experimental results show the feasibility and effectiveness of the proposed control strategy and the SVNPS-based power coordination control models.

INDEX TERMS Neural-like P system, state value, microgrid, power coordination.

I. INTRODUCTION

Currently, the energy source in electricity industry is gradually transferring from conventional to renewable, for a cleaner electrical power generation. Thus, plenty of renewable-based generators have been used in the electrical power systems. Photovoltaic (PV) generation is gaining popularity due to the characteristics of clean resource, continuous improvements in solar modules, and economic incentives from governments [1]. However, it is vulnerable to climate, which can arouse volatile, random, intermittent and uncontrolled output power. Therefore, energy storage equipment is of great importance to control power fluctuations and the research on power coordination control of the photovoltaic/battery microgird is urgently needed.

There are different characteristics and multiple operating modes (such as maximum power point tracking -MPPT-, constant power operation and operation stop) for PV generation units and energy storage units in a photovoltaic/battery microgrid. The logical relationship between different modes of energy storage units, such as charging and discharging modes, is complex. Once the logical relations can be clearly expressed and reasonably coordinated, the power regulation ability of microgrid will be improved significantly, as well as the reliability and economic benefit of

load power supply. There are two operation modes for a microgrid: grid–connected mode and isolated island operation mode [1], [2]. Dual characteristics coexist in units and loads when the microgrid is connected to grids, so that the power between units and loads are interacted via the Point of Common Coupling (PCC). Thus, the influence of the high penetration rate of photovoltaic distributed power generations (resulted from the randomness and volatility of the new energies) on the stability of the microgrid is considerable. Therefore, a reasonable and effective operation control strategy is essential for coordinating the output power of each unit in a microgrid as well as ensuring its operation stability. coordinated In [1], both microgrids operation models and unit statuses were established by Petri nets (PNs), and different algorithms for energy management were designed for distinguishing the operating characteristics in energy scheduling calculation. In [2], a cell–like fuzzy P system was proposed to establish the controlled units models of microgrids. The coordinated control and energy management were carried out by controlling units access or elimination. Moreover, multi–agent systems (MASs) were employed to construct the framework of microgrids through establishing the hierarchical agents with high performance. By studying inter-communications, specific functions and coordination strategies of agents, the operation control of microgrids was finally performed by dividing one task into several minor tasks to different agents by using MASs [3]–[7]. However, owing to the structure flexibility, changing operation modes and various distributed units with different characteristics in microgrids, the power coordinated control of microgrids is still a complicated and challenging work. Every method mentioned above has its own merits and demerits. For example, the control strategy based on PNs has the advantages of graphical knowledge representation and parallel information processing. However, the triggering condition and operation model definition are extremely complex. The cell-like fuzzy P system with fuzzy logic can make full use of expertise in a parallel manner, it can only control the unit access or elimination, but does not adjust the unit power output. In MASs, several agents are cooperated to fulfill the control strategy. Although the MAS-based distributed control coordination strategy for microgirids is attractive, the cooperation of different agents as well as the knowledge representation and behavior control of each agent are still unsolved. Therefore, particular attention should be paid to the modification and improvement of the aforementioned methods as well as the exploration of new ones for the power coordination control of microgirds.

A novel operation control strategy and power coordination control method for power systems using membrane systems (or P systems) [8] is discussed in this paper, which is attractive in computer science research [9], [10]. Membrane computing, a computing paradigm abstracted from the structure and function of living cells, is a new branch of natural computing. There are three types of membrane systems: *cell-like P systems*, *tissue-like P systems* and *neural-like P systems* (nP systems). *Spiking neural P systems* (SN P systems) and *basic neural-like P systems* (BnP systems) are included in the nP systems, where the SN P system is a fresh distribution and parallel neural computing device inspired by the neurophysiological behavior of neurons transmitting information by electrical impulses (spikes) along axons between neurons. The SN P system [11] is one of the important nP systems and has been proved with powerful computing ability in computing Turing computable functions [12], solving NP-complete problems in linear-time [13], generating binary and string languages [11], [12], and solving application problems, such as logic gates design [14], image processing [15], combinatorial optimization problem [16] and fault diagnosis [17]–[20].

The BnP systems are networks of neurons working with multisets (or strings) and conversing between different statuses [21]. They are inspired by the graphical structure and intercellular communication of biological neurons, and are special kinds of tissue-like P systems where the computational units (cells) are replaced by neurons. Therefore, the BnP system has excellent distributed parallel computing capability, covering characteristics of both *tissue-like P systems* and neuron systems. In [22], a simple neural-like P systems was proposed for improving the efficiency of maximum independent set selection in a distributed way. This neural-like P system is attractive because no information about the graph with overall size is needed for individual processors. In addition, the communication can be carried out with one-bit messages. Besides, by transmitting symbol-impulses (spikes) to neighboring neurons and processing multisets (or strings) of symbol–impulses (spikes) from the neighbors, the BnP system was improved to fulfill certain constraints in polynomial time without using neuron division or neuron separation [23]. Up to now, the research about BnP systems are still scattered. In the authors' opinion, the theoretical research and practical application of BnP system need to be further developed.

Actually, the BnP system with multisets (or strings) of objects and different states is suitable to describe the complex logical expressions of both different modes of PV units and statuses of energy storage units. A novel power coordination control strategy of microgrids based on the BnP systems is proposed in this article. A neural-like P system with state values (SVNPS) is defined based on the framework of the nP system. The state values (0 or 1) could be determined by comparing the objects in the neurons with thresholds, and the configuration of the SVNPS changes according to the corresponding values. In order to guarantee the operation stability of microgrids and avoid battery damage caused by fast/over charging/discharging, an operation control strategy based on PCC bus voltages and statuses of charge (SOC) of batteries is proposed. Based on the control strategy, the control power of the microgrid is decentralized into each unit by using the SVNPSs to construct the modes of microgrids units, and then the units can adjust the operation modes automatically according to the operation of the microgrid. Afterwards, the specific output power of the units will be reasonably

coordinated for operation stability of the microgrid. The proposed control strategy is implemented in MATLAB, and the experimental results show the efficiency improvement and the feasibility of unit SVNPSs model in microgrid power coordination.

The reminder of this paper is organized as follows. Section II describes the microgrid structure and declares the problem to be solved. Section III defines SVNPSs and each unit in the microgrid is modeled by the SVNPSs in Section IV. In Section V, the details about the simulation and the main results are presented. Conclusions are finally drawn in Section VI.

II. PROBLEM DESCRIPTION

A. STRUCTURE OF THE MICROGRID

The structure of the studied microgrid [2] is described in Figure 1, which contains a microgrid control center (MGCC), two photovoltaic generation units (PV units), an energy storage unit and loads (including static loads and adjustable loads).

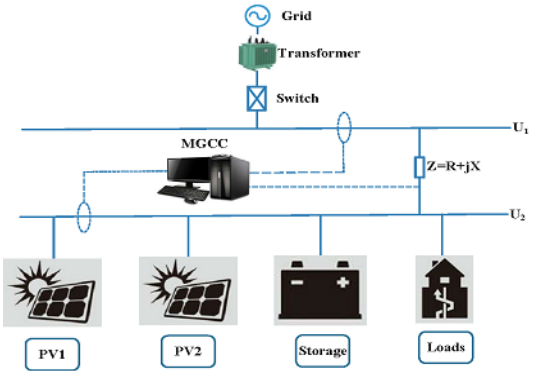

FIGURE 1. A sketch map of the studied PV/battery microgrid.

Due to the influence of light intensity and temperature, there could be a violent fluctuation and unfavorable discontinuity in the output power of PV units, which finally affects the stability of PPC bus voltage. In addition, load variation also affects the stability of PPC bus voltage. Therefore, it is necessary to ensure the operation stability of the microgrid according to real-time balance realization of the power.

In order to retard the batteries degradation caused by fast/over charging/discharging, SOC of batteries is limited in a reasonable range to control the charging/discharging power. According to different SOC ranges, five battery statuses are defined in Table 1, where P_{max} represents the upper limit of power.

When the PV/battery microgrid is connected to the grid, Equation (1) will be obtained based on voltage loss of transmission line

$$U_2 = U_1 - [R(-P_V + P_L \pm P_b) + X(-Q_V + Q_L \pm Q_b)]/U_2 \quad (1)$$

where: U_2 is PCC bus voltage connected to the front grid, U_1 is the grid voltage; P_V, P_L and P_b indicate the active power of PV, load and battery units, respectively; Q_V, Q_L and Q_b represent the reactive power of PV, load and battery units, respectively; R represents the line impedance and X represents the line reactance.

TABLE 1. Battery statuses and power limits of charging and discharging.

Storage unit status	Output power of storage	SOC lower limit	SOC upper limit	discharge power limit	charge power limit
VL	P1	0	10%	0	P_{max}
L	P2	10%	20%	$\frac{soc-soc10\%}{soc20\%-soc10\%} \times P_{max}$	P_{max}
M	P3	20%	80%	P_{max}	P_{max}
H	P4	80%	90%	P_{max}	$\frac{soc90\%-soc}{(soc90\%-soc80\%} \times P_{max}$
VH	P5	90%	100%	P_{max}	0

Noticing that the studied microgrid is in a medium and low voltage system and the impedance characteristic of the transmission lines is resistive. Thus, the reactive power related to the reactance X can be ignored. Therefore, PCC bus voltage depends on the active output power of PV, load and battery units. The active power shortage can be calculated by the voltage deviation, which is the difference between U_2 and MGCC with the rated voltage. The operation modes of each unit are determined by U_2 and SOC. Considering the active power shortage, predicted data of the PV units and loads, and the operation mode of each unit, the output active power of each unit is coordinated to ensure the stability of PCC bus voltage (within $\pm 5\%$ of the rated voltage) and microgrid power.

B. POWER COORDINATION CONTROL STRATEGY FOR PV/BATTERY SYSTEMS

In PV/battery microgrids, the power of loads and PV units is stochastic and fluctuant. Thus, energy storage units are used for power output complementation between loads and PV units. However, because of cost and limited capacity, energy storage unit is not always satisfactory. To solve this problem, an operation control strategy is proposed in this article based on PCC bus voltage and SOC of batteries considering load shedding and PV output power limit. The proposed strategy is shown in Figure 2 and the illustration of each variable is described in Table 2, where the charging and discharging power are restricted to protect the batteries.

When the microgrid is connected to the grid, the control strategy helps to stabilize PCC bus voltage within $\pm 5\%$ fluctuation of its rated voltage. The process is described as follows. Firstly, U_2 detected from MGCC is evaluated to see whether the amplitude of voltage is acceptable and the corresponding statuses of battery SOC could be obtained. There are five situations for a positive answer. According to the judgement result, the statuses of battery SOC are obtained. If the amplitude of U_2 is in the allowable range, there are five cases. (1) If U_2 fluctuates in a normal range and SOC is very low (VL), then PV units will work in MPPT mode and storage units will work in VL status, which means that batteries are

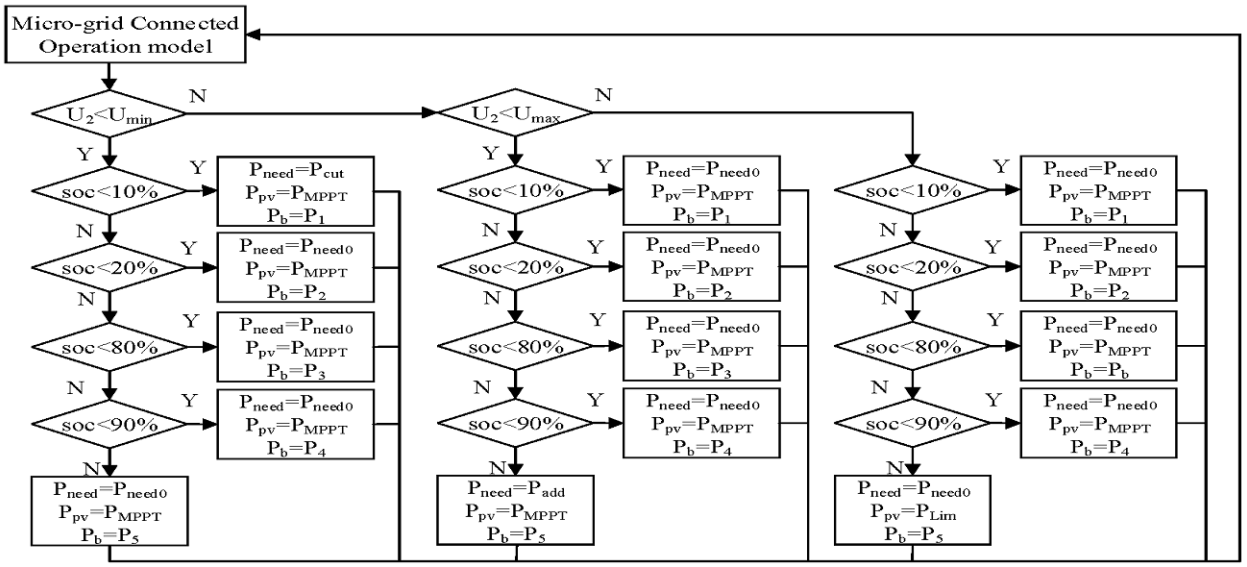

FIGURE 2. An operation control strategy.

TABLE 2. Variables and corresponding illustrations.

Variable	Illustration	Variable	Illustration
U_2	PCC point voltage	P_V	PV active power output
U_{min}	lower limit of PCC voltage fluctuation	P_{MPPT}	PV predictive active power
U_{max}	upper limit of PCC voltage fluctuation	$P_{\Delta V}$	PV active power increment
P_{need}	load active power output	P_{need0}	load predictive active power
P_b	battery predictive active power	P_{bmax}	PV battery maximum power

charged at maximum power while the discharging power is 0. (2) If SOC is low (L), then PV units will work in MPPT mode and storage units will work in L status, which means that batteries are charged at the maximum power while the discharging power is constrained. (3) If SOC is medium (M), then PV units will again work in MPPT mode and storage units will work in M status, which means that both the charging and discharging of batteries are at the maximum power. (4) If SOC is high (H), then PV units will again work in MPPT mode (maximize the use of clean energy) and storage units will work in H status, which means that the charge power of batteries are constrained while the discharging power is the maximum. (5) If SOC is very high (VH), then PV units will work in Lim and storage units will work in VH status, which means that the charge power is 0 while batteries are discharged at the maximum power.

In this study, the SVNPS is used to solve the operation mode conversion problem of each unit in the microgrid and state values in the SVNPSs are employed to represent the corresponding modes and statuses of different units. In what follows, the definition of the SVNPS is proposed in Section III, and then Section IV describes the modeling of SVNPSs for different units.

III. NEURAL-LIKE P SYSTEMS WITH STATE VALUES

A. BASIC NEURAL-LIKE P SYSTEMS

We recall the initial definition of BnP systems here as considered in [21]. The BnP systems are defined on the basis of tissue-like P systems, and the computational units are replaced by neurons. Such membrane systems contain multisets of objects, and each neuron is associated with states that can determine the operation of objects.

Definition 1: A BnP system (with degree $m \geq 1$) is a tuple

$$\Pi = (O, \sigma_1, \ldots, \sigma_m, syn, i_0)$$

where:

1) O is a finite non-empty alphabet (of chemical objects, but we also call them excitations/impulses);
2) $\sigma_1, \ldots, \sigma_m$ are neurons, of the form $\sigma_i = (Q_i, s_{i,0}, \omega_{i,0}, R_i)$, $1 \leq i \leq m$, where
   a) Q_i is a finite set (of states);
   b) $s_{i,0} \in Q_i$ is the initial state;
   c) $\omega_{i,0} \in O^*$ is the initial multiset of impulses contained in the neurons. Accordingly, $(s_{1,0}\omega_{1,0}, \ldots, s_{m,0}\omega_{m,0})$ is the initial configuration of Π;
   d) R_i is a finite set of rules of the form $s\omega \to s'xy_{go}z_{out}$, where $s, s' \in Q_i$, $\omega, x \in O^*$, $y_{go} \in (O \times \{go\})^*$, $z_{out} \in (O \times \{out\})^*$, with the restriction that $z_{out} = \lambda$ for all $i \in \{1, \ldots, m\}$ different from i_{out}; the mark go means that the associated impulses have to emit immediately and transmit to the linked neurons; the mark out means that the associated object outputs the system Π;
3) $syn \subseteq \{1, \ldots, m\} \times \{1, \ldots, m\}$ are synapses among neurons;
4) $i_0 \in \{1, \ldots, m\}$ indicates the set of indexes of output neurons.

B. NEURAL-LIKE P SYSTEMS WITH STATE VALUES

This paper proposes the neural-like P systems with state values (SVNPSs) in the framework of nP systems.

Definition 2: An SVNPS (with degree $m \geq 1$) is a tuple

$$\Pi = (O, T, Q, \sigma_1, \ldots, \sigma_m, \delta, \eta, syn, i_0)$$

where:

1) $O = \{d_1, \ldots d_q, d_{q+1}, \ldots, d_p\}$ is a finite alphabet whose elements are called *objects*, representing real variables. Objects in $O_{init} = \{d_1, \ldots, d_q\}$ are called *initial objects* and objects in $O_{fin} = \{d_{q+1}, \ldots, d_p\}$ are called *final objects*.
2) $T = \{\tau_{1,1}, \ldots, \tau_{1,r_1}, \ldots, \tau_{q,1}, \ldots, \tau_{q,r_q}\}$ is a finite set of real numbers (thresholds) associated with the set of initial objects O_{init}. Specifically, $\{\tau_{j,1}, \ldots, \tau_{j,r_j}\}$ are the thresholds associated with the initial object d_j in such manner that for each real value $v(d_j)$ of d_j, a vector of *state values* $(v_{j,1}, \ldots, v_{j,r_j})$ is defined as follows: for each k, $1 \leq k \leq r_j$,

$$v_{j,k} = \begin{cases} 0, & v(d_j) < \tau_{j,k} \\ 1, & v(d_j) \geq \tau_{j,k} \end{cases}$$

The vector of *state value* of $v(d_j)$ can be considered as a binary number with r_j digits.
3) $Q = \{s_1, \ldots, s_m\}$ is a finite alphabet such that $Q \cap O = \emptyset$ whose elements represent the statuses of the system in different moments ($s_1 \in Q$ denotes the initial status of the system). There exists a partition $\{Q_I, Q_F\}$ of $Q \backslash \{s_1\}$ such that the status in Q_I are called *intermediate status* and the status in Q_F are called *final status*.
4) $\sigma_1, \ldots, \sigma_m$ are the *neurons*, of the form $\sigma_i = (s_i, w_i, v_i, \mathcal{R}_i)$, where:
   - $s_i \in Q$ is the initial status of neuron σ_i. If $s_i \in Q_I$ (resp. $s_i \in Q_F$) then σ_i is called an *intermediate neuron* (resp. σ_i is an *output neuron*); σ_1 is called the *initial neuron*.
   - For the initial neuron, w_1 is a set of objects in O_{init} (the contents of σ_1) and v_1 is the empty-set. If σ_i is an intermediate neuron then w_i is the emptyset and v_i is a binary number representing some state values associated with σ_i (the contents of σ_i). If σ_i is an output neuron then w_i is a set of objects in O_{fin} (the contents of σ_i) and v_i is the emptyset.
   - $\mathcal{R}_i$ is a finite set of rules of type:
     - For the initial neuron: $s_1\ w_1 \rightarrow s_i v$, where $s_i \in Q_I$, $w_1 \subseteq O_{inic}$ and v is a set of vector of state values (binary numbers) corresponding to some real values of all objects in w_1.
     - For the intermediate neurons: $s_i v \rightarrow s_f w$, where $s_i \in Q_I$, $s_f \in Q_F$, v is a set of vector of state values corresponding to some real values of all objects in w_1, and $w \subseteq O_{fin}$ is a set of final objects.
     - For output neurons: $s_f w \rightarrow s_f(w, out)$, where $s_f \in Q_F$ and $w \subseteq O_{fin}$.
5) δ is a mapping from the set of all vectors of state values (binary numbers) corresponding to some real values of all objects in the initial neuron, onto the set Q_I of intermediate status of the system.
6) η is a mapping from the set of all vectors of state values (binary numbers) corresponding to some real values of all objects in the initial neuron, onto the cartesian product $Q_F \times O_{fin}$.
7) $syn \in \{1, \ldots, m\} \times \{1, \ldots, m\}$ such that for i, j, $1 \leq i, j \leq n$:
   - $(i, i) \notin syn$.
   - $(1, j) \in syn \Rightarrow s_j \in Q_I$.
   - $(i, j) \in syn \wedge s_i \in Q_I \Rightarrow s_j \in Q_F$.

   syn represents the *synapses* among neurons.
8) $i_0 \subseteq \{1, \ldots, m\}$ indicates the set of indexes of output neurons.

An overview of the computations is described as follows. An instantaneous description or a *configuration* C_t at an instant t of an SVNPS is described by the following pair: (a) the status of each neuron at instant t; (b) the contents (objects or binary numbers) of each neuron present in the system at that moment.

Given an assignment of real values $(v(d_1), \ldots, v(d_q))$ to the initial objects $d_1, \ldots, d_q$ in the initial neuron σ_1, the initial configuration associated with $(v(d_1), \ldots, v(d_q))$ is described by the following tuple: (a) the status of neuron σ_i is s_i; (b) the contents of the initial neuron σ_1 is $(v(d_1), \ldots, v(d_q))$; and (c) the contents of all intermediate neurons and all output neurons are the emptyset.

A rule $s_1\ w_1 \rightarrow s_i v$ for the initial neuron σ_1 fires when some real values $(v(d_1), \ldots, v(d_q))$ are assigned to all objects $d_1, \ldots d_q$ associated with σ_1. Then the corresponding vector of state values is $v = (v_{1,1}, \ldots, v_{1,r_1}, \ldots, v_{q,1}, \ldots, v_{q,r_q})$. When applying such a rule, the initial neuron σ_1 passes from status s_1 to status s_i, being $s_i = \delta(v_{1,1}, \ldots, v_{1,r_1}, \ldots, v_{q,1}, \ldots, v_{q,r_q})$, and the state values of vector v are sent to the intermediate neuron σ_i whose status is s_i.

A rule $s_i v \rightarrow s_f w$ for an intermediate neuron σ_i fires when σ_i receives the vector v of state values associated with some real values $(v(d_1), \ldots, v(d_q))$ assigned to all the initial objects $d_1, \ldots d_q$ in σ_1. When applying such a rule, the status of neuron σ_i changes from s_i to s_f, and the objects from w are produced and sent to the output neuron σ_f, being $\eta(v) = (s_f, w)$.

A rule $s_f w \rightarrow s_f(w, out)$ of an output neuron σ_f fires when σ_f receives the objects from w. When applying such a rule, the status of the system does not change, and the objects from w are released to the environment (the output ot the system). Then, the computation halts.

All computations of an SVNPS start from an initial configuration and proceed as stated above; only halting computations give a result, which is encoded by the objects present in the environment.

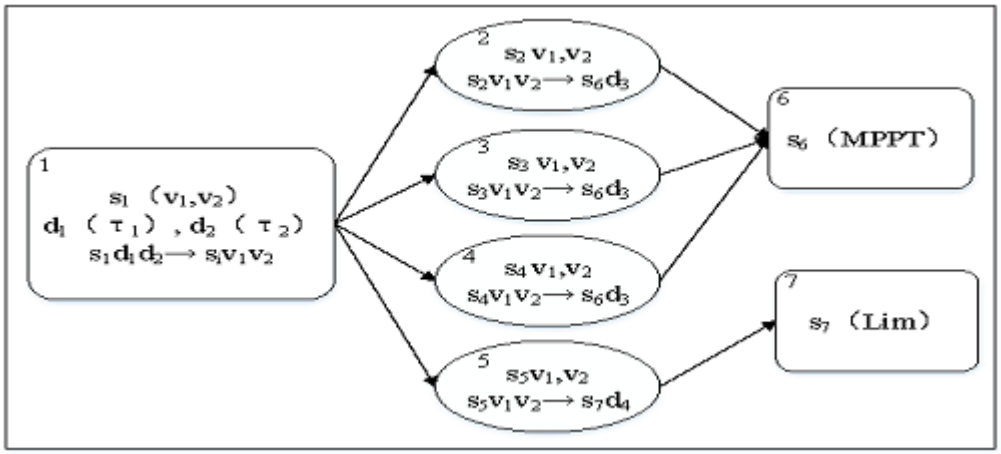

FIGURE 3. An SVNPS model for the PV unit.

IV. MODELLING FOR UNITS WITH SVNPSS

According to the operation control strategy presented in *subsection II-B* and the operation state of each unit, the unit SVNPS models are established and the control power of the microgrid operation is dispersed into each unit. Then the operation modes of each unit could be used to coordinate and control the output of each unit in the microgrid in a reasonable and efficient way, so as to meet the power balance and power quality output requirements of the microgrid.

A. SVNPS-BASED MODELS FOR MICROGRID UNITS

Since the neurons in SVNPSs contain multisets of objects and different statuses, an SVNPS can transform into different configurations by numerical comparison relationships between the objects and corresponding thresholds. The different statuses can be used to deal with the operation mode conversion in each unit of the microgrid. The operation modes and statuses of PV, storage and load units can be represented by the SVNPSs. Accordingly, the reliability of the control strategy is improved due to the distributed parallelism characteristics of SVNPSs. The SVNPS-based model for each unit is described in detail as follows.

1) AN SVNPS MODEL FOR THE PV UNIT

PV is clean energy, its output power is mainly affected by light intensity. To maximize economic benefits, PV units usually work in MPPT mode. According to the control strategy described in *subsection II-B*, if and only if U_2 is higher than the upper limit of allowable voltage fluctuation and the status of SOC is VH, then PV units work in the output power limiting status (Lim). Accordingly, an SVNPS-based model Π_1 for the PV unit is established, as shown in Figure 3.

An SVNPS-based model for a PV unit is a tuple $\Pi_1 = (O, T, Q, \sigma_1, \ldots, \sigma_m, \delta, \eta, syn, i_0)$, where:

- $O = \{d_1, d_2, d_3, d_4\}$, $O_{init} = \{d_1, d_2\}$, $O_{fin} = \{d_3, d_4\}$, where d_1 represents U_2, d_2 indicates SOC of batteries, d_3 describes MPPT mode and d_4 expresses Lim mode.
- $T = \{\tau_1, \tau_2\}$, where τ_1 is the threshold corresponding to d_1 and represents the upper limit of allowable voltage fluctuation; τ_2 is the threshold corresponding to d_2 and indicates the lower limit of battery SOC in the VH status.
- $Q = \{s_1, s_2, s_3, s_4, s_5, s_6, s_7\}$, $Q_I = \{s_2, s_3, s_4, s_5\}$, $Q_F = \{s_6, s_7\}$.
- $\sigma_1 = (s_1, w_1, v_1, \mathcal{R}_1)$, where: (a) $w_1 = \{d_1, d_2\}$; (b) $v_1 = \emptyset$; and (c) the rules from $\mathcal{R}_1$ are of type $s_1\, w_1 \rightarrow s_i v$, being $v \in \{0, 1\}^2$ representing the vector of state values associated with an assignment of real values $(v(d_1), v(d_2))$ to initial objects d_1, d_2. Table 3 shows the status and rules in each neuron.

TABLE 3. Neurons in SVNPS model for the PV unit.

Neuron	Status	Rule
σ_1	s_1, s_i	$\sigma_1 = (\{s_1(v_1, v_2)\}, \{d_1(\tau_1), d_2(\tau_2)\}, s_1 d_1 d_2 \rightarrow s)$
σ_2	s_2, s_6	$\sigma_2 = (\{s_2\,(v_1, v_2)\}, s_2 v_1 v_2 \rightarrow s_6 d_3)$
σ_3	s_3, s_6	$\sigma_3 = (\{s_3\,(v_1, v_2)\}, s_3 v_1 v_2 \rightarrow s_6 d_3)$
σ_4	s_4, s_6	$\sigma_4 = (\{s_4\,(v_1, v_2)\}, s_4 v_1 v_2 \rightarrow s_6 d_3)$
σ_5	s_5, s_6	$\sigma_5 = (\{s_5\,(v_1, v_2)\}, s_5 v_1 v_2 \rightarrow s_7 d_4)$
σ_6	s_6	$\sigma_6 = (s_6, d_3, \{s_6 d_3 \rightarrow s_6\,(d_3, out)\})$
σ_7	s_7	$\sigma_7 = (s_7, d_4, \{s_7 d_4 \rightarrow s_7\,(d_4, out)\})$

- For $2 \leq k \leq 5$, $\sigma_k = (s_k, w_k, v_k, \mathcal{R}_k)$, where: (a) $w_k = \emptyset$; (b) $v_k \in \{0, 1\}^2$ represents the vector of state values associated with an assignment of real values $(v(d_1), v(d_2))$ to initial objects d_1, d_2; and (c) the rules from $\mathcal{R}_k$ are of type $s_k v_k \rightarrow s_f w'_k$, being $\eta(v_k) = (s_f, w'_k)$.
- For $j = 6, 7$, $\sigma_j = (s_j, w_j, v_j, \mathcal{R}_j)$, where: (a) if $s_k v_k \rightarrow s_f w'_k$ is a rule of the intermediate neuron σ_k and $s_j = s_f$ then $w_j = w'_k$; (b) $v_j = \emptyset$; and (c) the rules from $\mathcal{R}_j$ are of type $s_j w_j \rightarrow s_j(w_j, out)$.
- δ is the mapping from $\{0, 1\}^2$ onto Q_I defined as follows: $\delta(0, 0) = s_2$, $\delta(0, 1) = s_3$, $\delta(1, 0) = s_4$ and $\delta(1, 1) = s_5$ (see Table 4).
- η is the mapping from $\{0, 1\}^2$ onto $Q_F \times O_{fin}$ defined as follows: $\eta(0, 0) = (s_6, d_3)$, $\eta(0, 1) = (s_6, d_3)$, $\eta(1, 0) = (s_6, d_3)$ and $\eta(1, 1) = (s_7, d_4)$.

TABLE 4. Relationships between state values and intermediate statuses in the SVNPS of PV units.

υ_2	υ_1	Status
0	0	s_2
0	1	s_3
1	0	s_4
1	1	s_5

– $syn = \{(1, 2), (1, 3), (1, 4), (1, 5), (2, 6), (3, 6), (4, 6), (5, 7)\}$.
– $i_0 = \{6, 7\}$.

There are seven neurons in the SVNPS Π_1, which means that it has seven statuses, *i.e.*, $s_1, \ldots, s_7$, where s_1 represents the initial status, $s_2, \ldots, s_5$ indicate intermediate statuses and s_6, s_7 describe final statuses. Accordingly, the output neurons are σ_6 and σ_7. The computing process of the SVNPS is described as follows.

Step 1: Calculate state values. There are objects d_1 and d_2 in neuron σ_1, and τ_1 and τ_2 represent the corresponding thresholds of the objects. By comparing d_1 with τ_1, the state value υ_1 is obtained. If $d_1 < \tau_1$, then $\tau_1 = 0$; otherwise, $\tau_1 = 1$. The state value υ_2 is obtained in a similar way;

Step 2: Choose intermediate statuses via the state values υ_2 and υ_1. The relationships between state values and intermediate statuses are shown in Table 4. The rules $s_1 d_1 d_2 \rightarrow s_i \upsilon_1 \upsilon_2$ in neuron σ_1 fire and the neuron changes from the initial status to an intermediate status, and then a state value $\upsilon_2\upsilon_1$ is sent to a corresponding neuron. For example, if $\upsilon_2\upsilon_1 = 00$, then the neuron changes to status s_2, which means that the value of $\upsilon_2\upsilon_1$ is sent to neuron σ_2;

Step 3: The rules in an intermediate neuron are fired when the neuron receives the state value, and the status of the neuron changes with producing and sending a new object to its postsynaptic neurons. For instance, if neuron σ_2 receives the value $\upsilon_2\upsilon_1$, then the rule $s_2\upsilon_1\upsilon_2 \rightarrow s_6 d_3$ in neuron σ_2 fires and a new object d_3 is produced and sent to neuron σ_6. Accordingly, the status of the neuron changes from s_2 to s_6;

Step 4: Termination conditions. The rules in an output neuron fire when the output neuron receives new objects and the computing of the SVNPS ends when the output neuron emits its objects. For example, the rule $s_6 d_3 \rightarrow s_6(d_3, out)$ in neuron σ_6 fires when the neuron receives the object d_3 from neuron σ_2 and the computing ends when d_3 is output from σ_6.

2) AN SVNPS MODEL FOR THE STORAGE UNIT

Batteries are with dual characteristic, which means that storage units in a microgrid can be used as a micro power to supply the loads or loads consuming electrical power. Thus, to avoid battery life damage caused by over/fast charging/discharging, the charging/discharging times and power should be limited. According to the different ranges of battery SOC, an SVNPS-based model Π_2 for the battery unit is built, as shown in Figure 4.

An SVNPS model for a battery unit is a tuple $\Pi_2 = (O, T, Q, \sigma_1, \ldots, \sigma_m, \delta, \eta, syn, i_0)$, where:

– $O = \{d_1, d_2, d_3, d_4, d_5, d_6, d_7\}$, $O_{init} = \{d_1, d_2\}$, $O_{fin} = \{d_3, d_4, d_5, d_6, d_7\}$, where d_1 represents U_2, d_2 indicates SOC of batteries, $d_3, d_4, \ldots, d_7$ express the five statues of the storage unit.

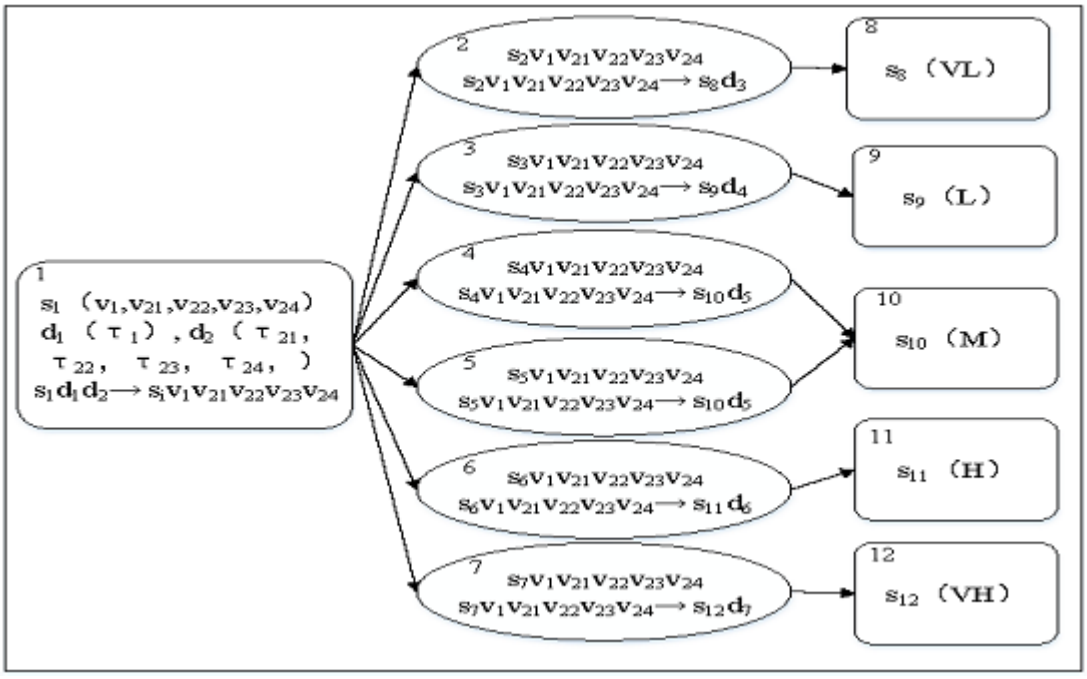

FIGURE 4. An SVNPS model for the battery unit.

TABLE 5. Neurons in SVNPS model for the battery unit.

Neuron	Status	Rule
σ_1	s_1, s_i	$\sigma_1 = (\{s_1(v_1, v_{21}, v_{22}, v_{23}, v_{24})\}, \{d_1(\tau_1), d_2(\tau_{21}, \tau_{22}, \tau_{23}, \tau_{24})\}, s_1 d_1 d_2 \rightarrow s_i v_1 v_{21} v_{22} v_{23} v_{24})$
σ_2	s_2, s_8	$\sigma_2 = (\{s_2(v_1, v_{21}, v_{22}, v_{23}, v_{24})\}, s_2 v_1 v_{21}, v_{22}, v_{23}, v_{24} \rightarrow s_8 d_3)$
σ_3	s_3, s_9	$\sigma_3 = (\{s_3(v_1, v_{21}, v_{22}, v_{23}, v_{24})\}, s_3 v_1 v_{21}, v_{22}, v_{23}, v_{24} \rightarrow s_9 d_4)$
σ_4	s_4, s_{10}	$\sigma_4 = (\{s_4(v_1, v_{21}, v_{22}, v_{23}, v_{24})\}, s_4 v_1 v_{21}, v_{22}, v_{23}, v_{24} \rightarrow s_{10} d_5)$
σ_5	s_5, s_{10}	$\sigma_5 = (\{s_5(v_1, v_{21}, v_{22}, v_{23}, v_{24})\}, s_5 v_1 v_{21}, v_{22}, v_{23}, v_{24} \rightarrow s_{10} d_5)$
σ_6	s_6, s_{11}	$\sigma_6 = (\{s_6(v_1, v_{21}, v_{22}, v_{23}, v_{24})\}, s_6 v_1 v_{21}, v_{22}, v_{23}, v_{24} \rightarrow s_{11} d_6)$
σ_7	s_7, s_{12}	$\sigma_7 = (\{s_7(v_1, v_{21}, v_{22}, v_{23}, v_{24})\}, s_7 v_1 v_{21}, v_{22}, v_{23}, v_{24} \rightarrow s_{12} d_7)$
σ_8	s_8	$\sigma_8 = (s_8, d_3, \{s_8 d_3 \rightarrow s_8 (d_3, out)\})$
σ_9	s_9	$\sigma_9 = (s_9, d_4, \{s_9 d_4 \rightarrow s_9 (d_4, out)\})$
σ_{10}	s_{10}	$\sigma_{10} = (s_{10}, d_5, \{s_{10} d_5 \rightarrow s_{10} (d_5, out)\})$
σ_{11}	s_{11}	$\sigma_{11} = (s_{11}, d_6, \{s_{11} d_1 \rightarrow s_{11} (d_6, out)\})$
σ_{12}	s_{12}	$\sigma_{12} = (s_{12}, d_7, \{s_{12} d_7 \rightarrow s_{12} (d_7, out)\})$

- $T = \{\tau_1, \tau_{21}, \tau_{22}, \tau_{23}, \tau_{24}\}$, where τ_1 is the threshold corresponding to d_1 and represents the upper limit of allowable voltage fluctuation; $\tau_{21}, \tau_{22}, \tau_{23}, \tau_{24}$ is the threshold corresponding to d_2 and indicates the lower limit of battery SOC in the L, M, H and VH statuses, respectively.
- $Q = \{s_1, s_2, \ldots, s_{12}\}$, $Q_I = \{s_2, s_3, \ldots, s_7\}$, $Q_F = \{s_8, s_9, \ldots, s_{12}\}$.
- $\sigma_1 = (s_1, w_1, v_1, \mathcal{R}_1)$, where: (a) $w_1 = \{d_1, d_2\}$; (b) $v_1 = \emptyset$; and (c) the rules from $\mathcal{R}_1$ are of type $s_1\, w_1 \rightarrow s_i v$, being $v \in \{0, 1\}^5$ representing the vector of state values associated with an assignment of real values $(v(d_1), v(d_2))$ to initial objects d_1, d_2. Table 5 shows the status and rules in each neuron.
- For $2 \leq k \leq 7$, $\sigma_k = (s_k, w_k, v_k, \mathcal{R}_k)$, where: (a) $w_k = \emptyset$; (b) $v_k \in \{0, 1\}^5$ represents the vector of state values associated with an assignment of real values $(v(d_1), v(d_2))$ to initial objects d_1, d_2; and (c) the rules from $\mathcal{R}_k$ are of type $s_k v_k \rightarrow s_f w'_k$, being $\eta(v_k) = (s_f, w'_k)$.
- For $8 \leq j \leq 12$, $\sigma_j = (s_j, w_j, v_j, \mathcal{R}_j)$, where: (a) if $s_k v_k \rightarrow s_f w'_k$ is a rule of the intermediate neuron σ_k and $s_j = s_f$ then $w_j = w'_k$; (b) $v_j = \emptyset$; and (c) the rules from $\mathcal{R}_j$ are of type $s_j w_j \rightarrow s_j(w_j, out)$.
- δ is the mapping from $\{0, 1\}^5$ onto Q_I defined as follows: $\delta(0, 0, 0, 0, 0) = s_2$, $\delta(0, 0, 0, 1, 0) = s_3$, $\delta(X, X, 1, 1, 0) = s_4$, $\delta(0, 0, X, X, 1) = s_5$, $\delta(0, 1, 1, 1, 1) = s_6$ and $\delta(1, 1, 1, 1, 1) = s_7$ (see Table 4). (Moreover, δ is not an injective function).
- η is the mapping from $\{0, 1\}^5$ onto $Q_F \times O_{fin}$ defined as follows: $\eta(0, 0, 0, 0, 0) = s_8$, $\eta(0, 0, 0, 1, 0) = s_9$, $\eta(X, X, 1, 1, 0) = s_{10}$, $\eta(0, 0, X, X, 1) = s_{10}$, $\eta(0, 1, 1, 1, 1) = s_{11}$ and $\eta(1, 1, 1, 1, 1) = s_{12}$. (Moreover, η is not an injective function).
- $syn = \{(1, 2), (1, 3), (1, 4), (1, 5), (1, 6), (1, 7), (2, 8), (3, 9), (4, 10), (5, 10), (6, 11), (7, 12)\}$.
- $i_0 = \{8, 9, 10, 11, 12\}$.

There are twelve neurons in the SVNPS Π_2, which means that it has twelve statuses, *i.e.*, $s_1, s_2, \ldots, s_{12}$, where s_1 indicates the initial status, $s_2, \ldots, s_7$ represent intermediate statuses and $s_8, \ldots, s_{12}$ describe terminated statuses. Accordingly, $\sigma_8, \ldots, \sigma_{12}$ are output neurons. The relationships between state values and intermediate statuses are shown in Table 6, where the character X means that the corresponding state value could be 0 or 1. The computing process of Π_2 is similar to Π_1 described in *Subsection IV-A-1)*.

TABLE 6. Relationships between state values and intermediate status in the SVNPS of storage units.

v_{24}	v_{23}	v_{22}	v_{21}	v_1	Status
0	0	0	0	0	s_2
0	0	0	1	0	s_3
X	X	1	1	0	s_4
0	0	X	X	1	s_5
0	1	1	1	1	s_6
1	1	1	1	1	s_7

3) AN SVNPS MODEL FOR THE LOAD UNIT

Loads include important and non-important loads. In the proposed SVNPS-based control strategy, the cutting in and cutting out of non-important loads are allowable to ensure continuous power supply for important loads and the maximum utilization of the energy, so as to guarantee the operation stability of the microgrid. If PCC bus voltage U_2 fluctuates in the allowable ranges and SOC of batteries is VH ($SOC > 90\%$), then the non-important loads cut in. If U_2 is lower than the allowed fluctuation voltage ($U_2 < 90\%$ rated voltage) and SOC of batteries is VL ($SOC < 10\%$), the non-important loads cut out. In other cases, the cutting in/out of loads is not considered. An SVNPS-based model Π_3 for the load unit is established, as shown in Figure 5. The relationships between state values and intermediate statuses are shown in Table 7. The computing process of Π_3 is similar to Π_1 described in *Subsection IV-A-1)*.

An SVNPS model for a load unit is a tuple $\Pi_3 = (O, T, Q, \sigma_1, \ldots, \sigma_m, \delta, \eta, syn, i_0)$, where:

- $O = \{d_1, d_2, d_3, d_4, d_5\}$, $O_{init} = \{d_1, d_2\}$, $O_{fin} = \{d_3, d_4, d_5\}$,, where d_1 represents U_2, d_2 indicates SOC of batteries, d_3, d_4, d_5 express the three statuses of the load unit.
- $T = \{\tau_{11}, \tau_{12}, \tau_{21}, \tau_{22}\}$, where $\tau_{11}\tau_{12}$ is the threshold corresponding to d_1, τ_{11} and τ_{12} represent the upper and lower limit of allowable voltage fluctuation, respectively; $\tau_{21}\tau_{22}$ is the threshold corresponding to d_2, τ_{21} and τ_{22} indicate the lower limit of battery SOC in the L and VH statuses, respectively.
- $Q = \{s_1, s_2, \ldots, s_9\}$, $Q_I = \{s_2, s_3, \ldots, s_6\}$, $Q_F = \{s_7, s_8, s_9\}$.
- $\sigma_1 = (s_1, w_1, v_1, \mathcal{R}_1)$, where: (a) $w_1 = \{d_1, d_2\}$; (b) $v_1 = \emptyset$; and (c) the rules from $\mathcal{R}_1$ are of type $s_1\, w_1 \rightarrow s_i v$, being $v \in \{0, 1\}^4$ representing the vector of state values associated with an assignment of real values

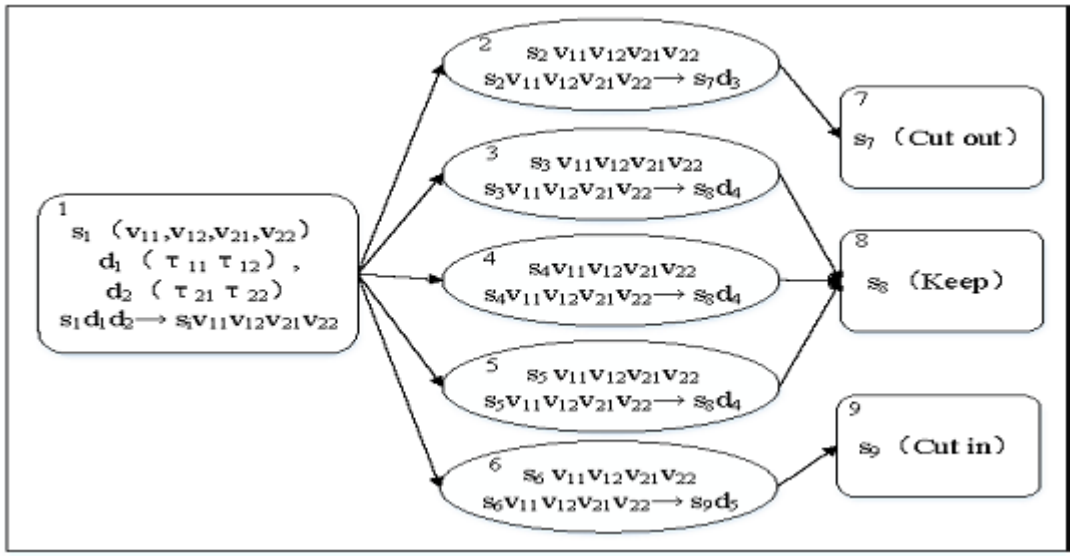

FIGURE 5. An SVNPS model for the load unit.

TABLE 7. Relationships between state values and intermediate status in the SVNPS of load units.

v_{22}	v_{21}	v_{12}	v_{11}	Status
1	1	0	1	s_2
X	1	0	0	s_3
0	X	0	1	s_4
X	X	1	1	s_5
0	0	0	0	s_6

TABLE 8. Neurons in SVNPS model for the load unit.

Neuron	Status	Rule
σ_1	s_1, s_i	$\sigma_1 = (\{s_1(v_{11}, v_{12}, v_{21}, v_{22})\}, \{d_1(\tau_{11}, \tau_{12}), d_2(\tau_{21}, \tau_{22})\}, s_1 d_1 d_2 \rightarrow s_i v_{11} v_{12} v_{22} v_{21} v_{22})$
σ_2	s_2, s_7	$\sigma_2 = (\{s_2(v_{11}, v_{12}, v_{21}, v_{22})\}, s_2 v_{11} v_{12} v_{21} v_{22} \rightarrow s_7 d_3)$
σ_3	s_3, s_8	$\sigma_3 = (\{s_3(v_{11}, v_{12}, v_{21}, v_{22})\}, s_3 v_{11} v_{12} v_{21} v_{22} \rightarrow s_8 d_4)$
σ_4	s_4, s_8	$\sigma_4 = (\{s_4(v_{11}, v_{12}, v_{21}, v_{22})\}, s_4 v_{11} v_{12} v_{21} v_{22} \rightarrow s_8 d_4)$
σ_5	s_5, s_8	$\sigma_5 = (\{s_5(v_{11}, v_{12}, v_{21}, v_{22})\}, s_5 v_{11} v_{12} v_{21} v_{22} \rightarrow s_8 d_4)$
σ_6	s_6, s_9	$\sigma_6 = (\{s_6(v_{11}, v_{12}, v_{21}, v_{22})\}, s_6 v_{11} v_{12} v_{21} v_{22} \rightarrow s_9 d_5)$
σ_7	s_7	$\sigma_7 = (s_7, d_3, \{s_7 d_3 \rightarrow s_7 (d_3, out)\})$
σ_8	s_8	$\sigma_8 = (s_8, d_3, \{s_8 d_3 \rightarrow s_8 (d_3, out)\})$
σ_9	s_9	$\sigma_9 = (s_9, d_5, \{s_9 d_5 \rightarrow s_9 (d_5, out)\})$

$(v(d_1), v(d_2))$ to initial objects d_1, d_2. Table 8 shows the status and rules in each neuron.

- For $2 \leq k \leq 6$, $\sigma_k = (s_k, w_k, v_k, \mathcal{R}_k)$, where: (a) $w_k = \emptyset$; (b) $v_k \in \{0, 1\}^4$ represents the vector of state values associated with an assignment of real values $(v(d_1), v(d_2))$ to initial objects d_1, d_2; and (c) the rules from $\mathcal{R}_k$ are of type $s_k v_k \rightarrow s_f w'_k$, being $\eta(v_k) = (s_f, w'_k)$.
- For $7 \leq j \leq 9$, $\sigma_j = (s_j, w_j, v_j, \mathcal{R}_j)$, where: (a) if $s_k v_k \rightarrow s_f w'_k$ is a rule of the intermediate neuron σ_k and $s_j = s_f$ then $w_j = w'_k$; (b) $v_j = \emptyset$; and (c) the rules from $\mathcal{R}_j$ are of type $s_j w_j \rightarrow s_j(w_j, out)$.
- δ is the mapping from $\{0, 1\}^4$ onto Q_I defined as follows: $\delta(1, 1, 0, 1) = s_2$, $\delta(X, 1, 0, 0) = s_3$, $\delta(0, X, 0, 1) = s_4$, $\delta(X, X, 1, 1) = s_5$ and $\delta(0, 0, 0, 0) = s_6$ (see Table 6). (Moreover, δ is not an injective function).
- η is the mapping from $\{0, 1\}^4$ onto $Q_F \times O_{fin}$ defined as follows: $\eta(1, 1, 0, 1) = s_7$, $\eta(X, 1, 0, 0) = s_8$, $\eta(0, X, 0, 1) = s_8$, $\eta(X, X, 1, 1) = s_8$ and $\eta(0, 0, 0, 0) = s_9$. (Moreover, η is not an injective function).
- $syn = \{(1, 2), (1, 3), (1, 4), (1, 5), (1, 6), (2, 7), (3, 8), (4, 8), (5, 8), (6, 9)\}$.
- $i_0 = \{7, 8, 9\}$.

B. POWER COORDINATION CONTROL BASED ON SVNPSS

The out power of each unit is associated with not only PCC bus voltage and SOC, but also the statuses of other units in the same microgrid. Thus, PCC bus voltage, SOC and statuses of all the units should be considered to fulfill power coordination control. The operation modes and statuses of each unit can be obtained via the SVNPS-based models (Π_1, Π_2, Π_3) built in *Subsection IV-A*. However, the specific output power of each unit is still unknown. So, this section aims at setting the power output rules of each unit for power coordination control considering operation stability of the microgrid. The flow chart of power coordination is shown in Figure 6, where charging/discharging rules of batteries are shown in Figure 7.

Next, main steps in Figure 6 is described as follows. Firstly, the active power shortage $\triangle P$ is calculated via PCC bus voltage. In this paper, it is agreed that the positive direction of power flow is from the microgrid to the connected grid. Thus, $\triangle P > 0$ means that U_2 is higher than the rated voltage and there is superfluous electricity in the microgrid. In this

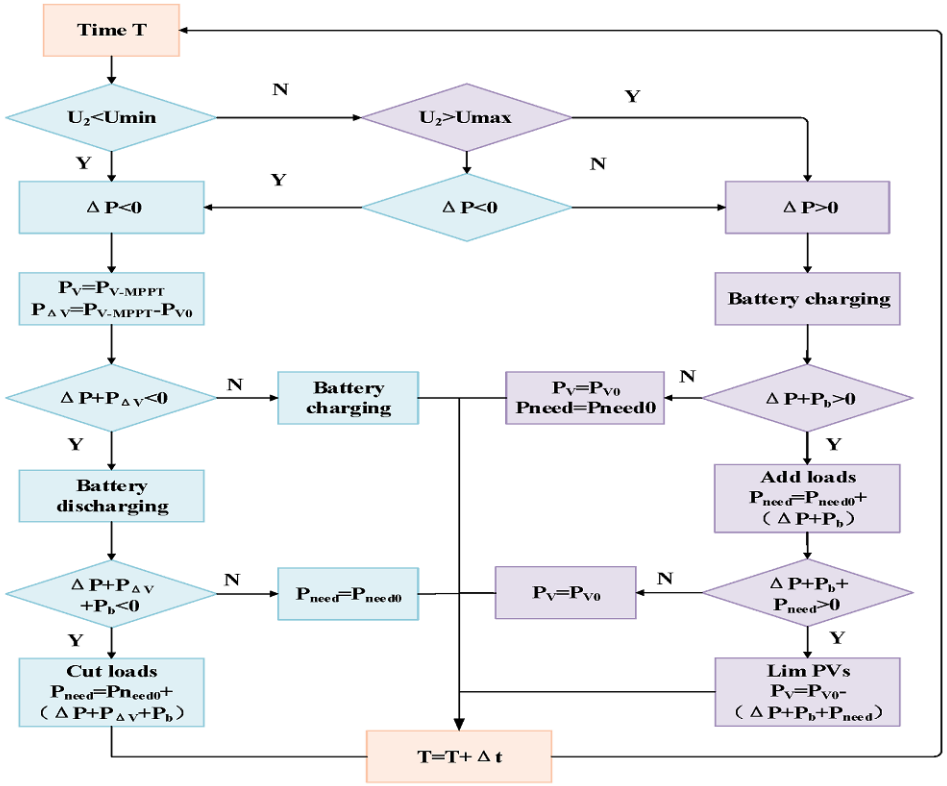

FIGURE 6. The flow chart of power coordination.

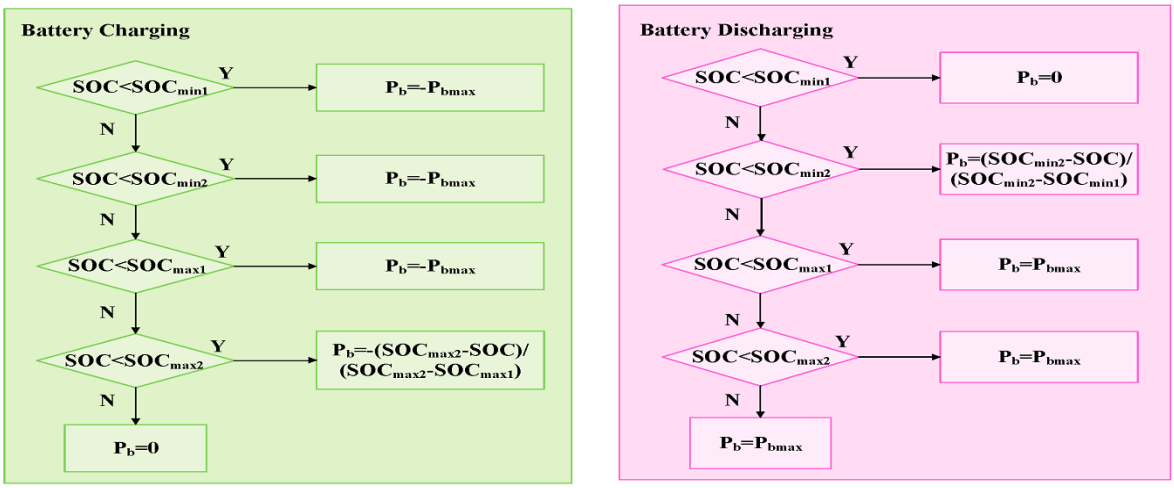

FIGURE 7. The principle for charging and discharging of batteries.

case, batteries charge according to the status of SOC. If SOC is high and the redundant power $\triangle P$ cannot be absorbed by batteries, then non-important loads are cut in to consume the electricity. After that, if $\triangle P$ still cannot be fully absorbed, then PV power generation is limited to balance the power in the microgird. Likewise, $\triangle P < 0$ means that U_2 is lower than the rated voltage and there is an electricity shortage in the interior of the microgrid. In this case, it is needed to increase the power supply of PV and storage units. If a PV unit works in the Lim status, then it should immediately switch to work in MPPT mode. After that, if the power shortage is not solved, then the storage units discharge to supply power. Besides, if necessary, non-important loads could be cut out to ensure power coordination of the microgrid.

V. SIMULATION AND ANALYSIS

This section displays the simulation and validation of the proposed control strategy, as well as the comparison results with

two other control strategies, i.e., traditional control strategy without storage and traditional control strategy with storage.

A. TRADITIONAL CONTROL STRATEGY WITHOUT STORAGE

The capacity parameters of microgrid units are shown in Table 9. The output power of PV and load units in Figure 8 are used to predict the power of a typical summer day (from 10 am to 18 pm). Figure 9 is PCC voltage fluctuation curve when the microgrid only contains PV and load units. In this situation, the PCC point voltage can be calculated by Equation (1). In Figure 9, it can be seen that there is an intense voltage fluctuation (beyond ±5% of the rated voltage), which will cause damage on the loads and affect the operation stability of the microgrid.

TABLE 9. Capacity parameters of microgrid units.

PV1/kW	PV2/kW	Storage/kWh	Load1/kW	Load2/kW
30	30	60	30	15

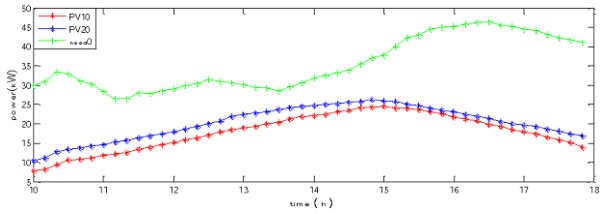

FIGURE 8. Output power of PVs and loads.

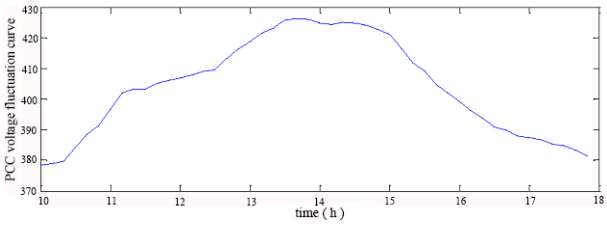

FIGURE 9. PCC voltage fluctuation curve.

B. TRADITIONAL CONTROL STRATEGY WITH STORAGE

Storage units could be used to control the stability of the microgrid instantaneous power. The output power, loads and batteries under this control strategy are plotted in Figure 10. Working in MPPT mode is beneficial to improve the energy efficiency for PV generation units. The initial value of battery SOC is 75%, and the maximum charging/discharging power of storage unit is 45kW.

The charging of SOC can be seen in Figure 11. In time periods, from 10:00 am to 10:40 am and from 17:00 pm to 18:00 pm, PV power generation is low but the load demand is high. Thus, battery discharging is needed to meet the power supply. In this situation, the battery output power is positive and there is a downward trend of SOC. In time period, from 10:40 am to 12:00 pm, the storage unit is 0 and there is no charging for battery. In time period, from

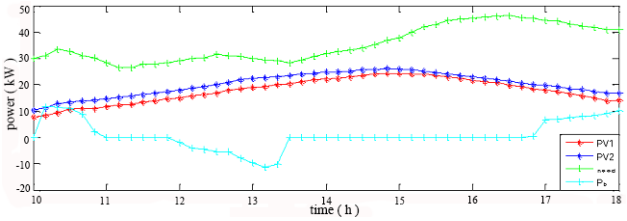

FIGURE 10. Output power of PVs, loads and batteries.

12:00 pm to 13:10 pm, due to the enhancement of light intensity, PV units provide excessive electricity and the battery is fully charged. After that, the system voltage will be high because of the power generation redundancy.

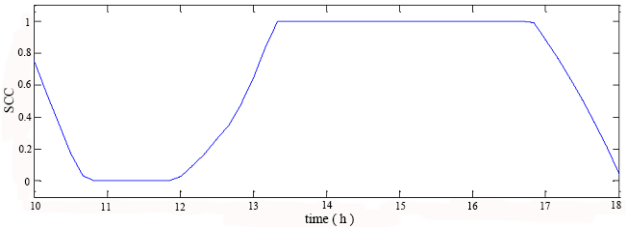

FIGURE 11. SOC change curve.

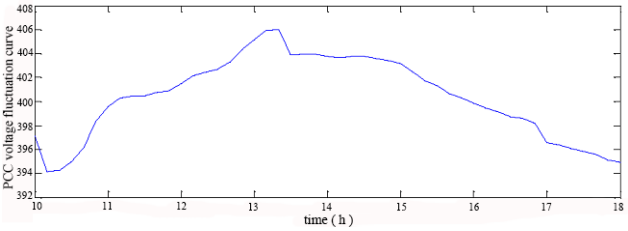

FIGURE 12. PCC voltage fluctuation curve.

The PCC voltage fluctuation curve is shown in Figure 12. It indicates that the instantaneous power of the microgird can be smoothed by the storage unit. However, there is still a fierce voltage fluctuation due to the limited battery capacity. Besides, frequency charging/discharging, empty or full voltage of SOC will result in a reduction of battery life.

C. OPERATION CONTROL STRATEGY BASED ON SVNPSS

The experiments based on the proposed strategy with SVNPSs are shown in Figures 13 to 15. Figure 13 displays the power changing curves of polysilicon photovoltaic, monocrystalline silicon photovoltaic, loads and batteries. Figure 14 indicates the changing curve of SOC. Figure 15 is the result of the voltage fluctuation curve of PCC bus.

During time period 10 am to 11 am, PV power generation is low, whereas the load demand and SOC of batteries are high. In this case, the batteries discharge to supply power, the output power of the batteries is positive and SOC has a downward trend. It should be mentioned that, because of the limitation on battery discharging power, this downward trend is slower than that under traditional control strategy.

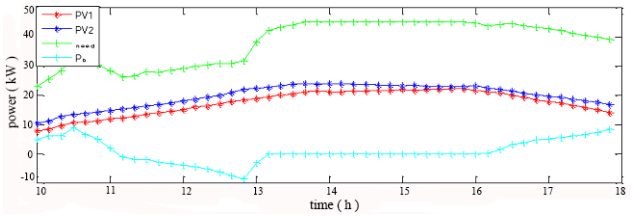

FIGURE 13. Power change curves of PVs, loads and batteries.

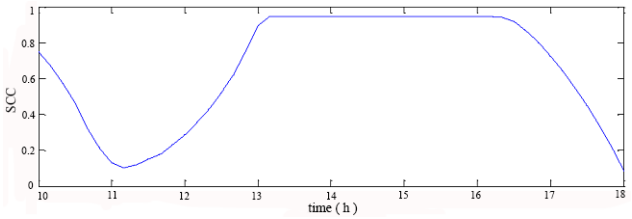

FIGURE 14. SOC change curve.

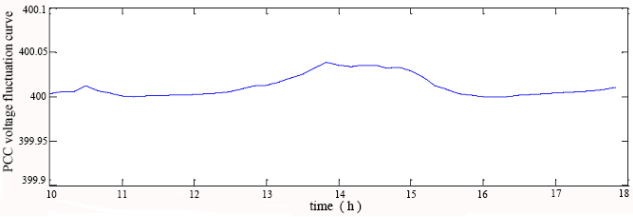

FIGURE 15. PCC voltage fluctuation curve.

From 11 am to 13 pm, the output power of PVs increases due to the enhancement of light intensity. At this moment, batteries will be charged from the excessive power. The output is negative and SOC displays an upward trend. At 13:15 pm, the microgird still has power excess while SOC reaches saturation state, which means that the batteries cannot be recharged. Therefore, the loads are cut in to balance the power. At 13:45 pm, the PV units are limited because there is still excess of power after adding all the loads. At 16:00 pm, the PV units are switched from limited mode to MPPT mode since the PV power generation decreases with the weakening light. Subsequently, the loads increase but the power cannot be balanced with MPPT mode. In this condition, the batteries will discharge and SOC will decrease. Figure 15 indicates that the control strategy based on PCC bus voltage and SOC is favorable to power balance of each unit and system voltage quality.

The results, from Figures 8 to 15, with different control strategies reveal that storage units can improve the active power balance to some extent. However, there is still a violent fluctuation in PCC bus voltage. The proposed SVNPS-based control strategy can overcome this shortcoming and has the following advantages: 1) adjusting output power of loads and PVs, and 2) providing battery protection with a power limit. Besides, the SVNPS offers an intuitive illustration based on a strictly mathematical expression and provides a graphical and parallel way for describing the complex modes and statuses of PV and storage units.

VI. CONCLUSIONS

An SVNPS is proposed in this article, and state values in the SVNPS are used for system switching to different configurations. Based on the SVNPS, an operation control strategy of microgirds is presented to coordinate the power. The SVNPS is used to deal with the multi-modes of different units in the microgird by constructing unit SVNPS-based models and then the output power is coordinated according to the operation statuses of the constructed SVNPSs. Finally, simulations with different control strategies, i.e., traditional control strategy without storage, traditional control strategy with storage and operation control strategy based on SVNPSs, are performed to validate the capability of the proposed strategy. The objective of this article is proposing a new control strategy and verifying the feasibility and effectiveness of the presented method. In the future, works will be carried out to prove the superiority of SVNPSs for energy management of complex microgrids.

ACKNOWLEDGMENT

The authors would like to express special gratitude to Dr. Luis Valencia Cabrera for some useful discussions in preparing this paper.

REFERENCES

[1] D. Lu, H. Fakham, T. Zhou, and B. François, "Application of Petri nets for the energy management of a photovoltaic based power station including storage units," *Renew. Energy*, vol. 35, no. 6, pp. 1117–1124, Jun. 2010.

[2] J. Wang, K. Chen, M. Li, M. Ming, P. Jun, and H. Peng, "Cell-like fuzzy P system and its application in energy management of micro-grid," *J. Comput. Theor. Nanosci.*, vol. 13, no. 6, pp. 3643–3651, Jun. 2016.

[3] M. W. Khan and J. Wang, "The research on multi-agent system for microgrid control and optimization," *Renew. Sustain. Energy Rev.*, vol. 80, pp. 1399–1411, Dec. 2017.

[4] A. L. Dimeas and N. D. Hatziargyriou, "Operation of a multiagent system for microgrid control," *IEEE Trans. Power Syst.*, vol. 20, no. 3, pp. 1447–1455, Aug. 2005.

[5] V.-H. Bui, A. Hussain, and H.-M. Kim, "A multiagent-based hierarchical energy management strategy for multi-microgrids considering adjustable power and demand response," *IEEE Trans. Smart Grid*, vol. 9, no. 2, pp. 1323–1333, Mar. 2018.

[6] R. de Azevedo, M. H. Cintuglu, T. Ma, and O. A. Mohammed, "Multiagent-based optimal microgrid control using fully distributed diffusion strategy," *IEEE Trans. Smart Grid*, vol. 8, no. 4, pp. 1997–2008, Jul. 2017.

[7] V.-H. Bui, A. Hussain, and H.-M. Kim, "Optimal operation of microgrids considering auto-configuration function using multiagent system," *Energies*, vol. 10, no. 10, p. 1484, Sep. 2017.

[8] G. Paŭn, "Computing with membranes," *J. Comput. Syst. Sci.*, vol. 61, no. 1, pp. 108–143, Aug. 2000.

[9] T. Wang, G. Zhang, J. Zhao, Z. He, J. Wang, and M. J. Pérez-Jiménez, "Fault diagnosis of electric power systems based on fuzzy reasoning spiking neural P systems," *IEEE Trans. Power Syst.*, vol. 30, no. 3, pp. 1182–1194, May 2015.

[10] T. Wang, G. Zhang, and M. J. Pérez-Jiménez, "Fuzzy membrane computing: Theory and applications," *Int. J. Comput. Commun*, vol. 10, no. 6, pp. 861–892, Oct. 2015.

[11] M. Ionescu, G. Păun, and T. Yokomori, "Spiking neural P systems," *Fundam. Inf.*, vol. 71, no. 2, pp. 279–308, Jan. 2006.

[12] X. Zeng, L. Xu, X. Liu, and L. Pa, "On languages generated by spiking neural P systems with weights," *Inf. Sci.*, vol. 278, no. 10, pp. 423–433, Sep. 2014.

[13] T. Pan, X. Shi, Z. Zhang, and F. Xu, "A small universal spiking neural P system with communication on request," *Neurocomputing*, vol. 275, pp. 1622–1628, Jan. 2017.

[14] T. Song, P. Zheng, M. L. Wong, and X. Wang, "Design of logic gates using spiking neural P systems with homogeneous neurons and astrocytes-like control," *Inf. Sci.*, vol. 372, no. 1, pp. 380–391, Dec. 2016.
[15] D. Díaz-Pernil, F. Peña-Cantillana, and M. A. Gutiérrez-Naranjo, "A parallel algorithm for skeletonizing images by using spiking neural P systems," *Neurocomputing*, vol. 115, no. 4, pp. 81–91, Sep. 2013.
[16] G. Zhang, H. Rong, F. Neri, and M. J. Pérez-Jiménez, "An optimization spiking neural P system for approximately solving combinatorial optimization problems," *Int. J. Neural Syst.*, vol. 24, no. 5, p. 1440006, Aug. 2014.
[17] H. Peng, J. Wang, M. J. Pérez-Jiménez, H. Wang, J. Shao, and T. Wang, "Fuzzy reasoning spiking neural P system for fault diagnosis," *Inf. Sci.*, vol. 235, pp. 106–116, Jun. 2013.
[18] G. Xiong, D. Shi, L. Zhu, and X. Duan, "A new approach to fault diagnosis of power systems using fuzzy reasoning spiking neural P systems," *Math. Problems Eng.*, vol. 2013, May 2013, Art. no. 815352.
[19] Y. Y. He, T. Wang, K. Huang, G. X. Zhang, and M. J. Pérez-Jiménez, "Fault diagnosis of metro traction power systems using a modified fuzzy reasoning spiking neural P system," *Romanian J. Inf. Sci. Technol.*, vol. 18, no. 3, pp. 256–272, Jan. 2015.
[20] H. Peng *et al.*, "Fault diagnosis of power systems using intuitionistic fuzzy spiking neural P systems," *IEEE Trans. Smart Grid*, to be published, doi: 10.1109/TSG.2017.2670602.2017.
[21] J. Pazos, A. Rodríguez-Patón, and A. Silva, "Solving SAT in linear time with a neural-like membrane system," *Lect. Notes Comput. Sci.*, vol. 2686, pp. 662–669, Jun. 2003.
[22] L. Xu and P. Jeavons, "Simple neural-like p systems for maximal independent set selection," *Neural Comput.*, vol. 25, no. 6, pp. 1642–1659, Jun. 2013.
[23] L. Xu, X. Zeng, and P. Jeavons, "A polynomial-time solution to constraint satisfaction problems by neural-like P systems," *Int. J. Unconventional Comput.*, vol. 9, nos. 5–6, pp. 465–481, Jan. 2013.

TAO WANG received the Ph.D. degree in electrical engineering from the Southwest Jiaotong University, Chengdu, China, in 2016. She was a Visiting Student in the Computer Science and Artificial Intelligence with the University of Sevilla, Sevilla, Spain, from 2013 to 2014. She has been currently a Lecturer with the School of Electrical Engineering and Electronic Information, Xihua University, since 2016. Her research interests include microgrid energy management, fault diagnosis, membrane computing, and bio-inspired model theory and its application in electrical power system.

JUN WANG received the Ph.D. degree in electrical engineering from Southwest Jiaotong University, China, in 2006. She was a Lecturer with the Sichuan College of Science and Technology, China, from 1991to 2003 and an Associate Professor with Xihua University, China, from 1998to 2003. She has been currently a Professor with the School of Electrical and Information Engineering, Xihua University, China, since 2004. Her research interests include electrical automation, intelligent control, and membrane computing.

JUN MING received the M.A. degree in electrical engineering from Xihua University, Chengdu, China, in 2018. She is currently with the State Grid Zigong Electric Power Supply Company. Her research interests include membrane computing and microgrid energy management.

ZHANG SUN received the M.A. degree in power electronics and power transmission from Xihua University. He is currently pursuing the Ph.D. degree in electrical engineering with Southwest Jiaotong University, Chengdu, China. He is currently a Lecturer with the School of Electrical Engineering and Electronic Information, Xihua University. His research interests include distributed generation and microgrid energy management.

CHUANXIANG WEI received the M.A. degree in electrical engineering from Xihua University, Chengdu, China. He is currently with State Grid Nanchong Electric Power Supply Company. His research interests include distributed generation.

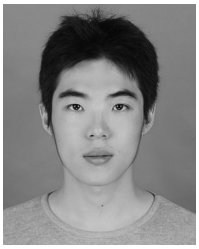

CHUN LU received the M.A. degree in transportation engineering from Southwest Jiaotong University, Chengdu, China, in 2015. He is currently pursuing the Ph.D. degree in mechanical engineering with Ceit and Tecnun, University of Navarra, Spain. His research interests include bio-inspired model theory and its application, signal diagnosis, system dynamics, and railway engineering.

MARIO J. PÉREZ-JIMÉNEZ received the degree in mathematics from University of Barcelona and the Ph.D. degree in mathematics from Sevilla University. In the past, he was a Lecturer and a Teaching Assistant with the University of Barcelona. He is currently a Full Professor with the Department of Computer Science and Artificial Intelligence. From 2005 to 2007, he was a Guest Professor with the Huazhong University of Science and Technology, Wuhan, China. He is also a numerary member of the Academia Europaea (The Academy of Europe) in the Section of Informatics. He is currently the Head of the Research Group on Natural Computing, University of Sevilla. He has supervised 14 doctoral theses. His main research interests include theory of computation, computational complexity theory, natural computing (DNA computing and membrane computing), bioinformatics, and computational modeling for complex systems. He has published 19 books in computer science and mathematics, and over 300 scientific papers in international journals (collaborating with researchers worldwide). He is a member of the Editorial Board of six ISI journals. He has been the first scientific awarded with—Important Contributions to Membrane Computing under the auspices of the European Molecular Computing Consortium, Edinburgh, in 2008. In 2014, he received the University of Sevilla FAMA Award for his outstanding research career. He is the main researcher in various European, Asian, Spanish, and Andalusian research grants. From 2003, he was an expert-reviewer of the Prospective and Evaluation National Agency of Spain. From 2006, he was an European Science Foundation peer reviewer, from 2008, he was an expert reviewer of the Romanian National University Research Council, and from 2015, he was an international expert from the Russian Science Foundation, invited by the Russian International Affairs Council.